MODELING AND ANALYSIS OF STRUCTURAL DYNAMICS FOR A ONE-TENTH SCALE MODEL NGST SUNSHIELD

John Johnston[1] and Sebastien Lienard[2]

[1]NASA Goddard Space Flight Center, Greenbelt, MD

[2]Ideamech SAS, 10 Avenue de l'Europe - 31520 Ramonville Saint Agne – France

Abstract

New modeling and analysis techniques have been developed for predicting the dynamic behavior of the NGST sunshield. The sunshield consists of multiple layers of pretensioned, thin-film membranes supported by deployable booms. Modeling the structural dynamic behavior of the sunshield is a challenging aspect of the problem due to the effects of membrane wrinkling. A finite element model of the sunshield was developed using an approximate engineering approach, the cable network method, to account for membrane wrinkling effects. Ground testing of a one-tenth scale model of the NGST sunshield were carried out to provide data for validating the analytical model. A series of analyses were performed to predict the behavior of the sunshield under the ground test conditions. Modal analyses were performed to predict the frequencies and mode shapes of the test article and transient response analyses were completed to simulate impulse excitation tests. Comparison was made between analytical predictions and test measurements for the dynamic behavior of the sunshield. In general, the results show good agreement with the analytical model correctly predicting the approximate frequency and mode shapes for the significant structural modes.

Introduction

The Next Generation Space Telescope (NGST) will feature a lightweight, deployable sunshield for passive cooling of its optics. The sunshield consists of multiple layers of pretensioned, thin-film membranes that are supported by deployable booms. The structural dynamics of the sunshield are a concern due to the strict line-of-site jitter requirements of the telescope. Structural modeling and analysis techniques must accurately characterize sunshield modes having significant modal mass participation to ensure that they will be filtered by the Spacecraft's ACS and/or any added vibration isolation system such that they will not impair the pointing performance of the telescope. The recently cancelled Inflatable Sunshield In Space (ISIS) flight experiment[1-3] was to validate the deployment of a one-third scale NGST sunshield in space and provide data for correlation of analytical models. As part of the ISIS project, an additional subscale NGST sunshield test article was fabricated for use in ground dynamic testing. This paper discusses the modeling and analysis efforts underway in support of the one-tenth scale model ground dynamic testing. First, a discussion of sunshield dynamics modeling is presented. A summary of the one-tenth scale model NGST sunshield ground dynamic tests is then presented. Next, an analysis of the experiments is presented. Finally, a comparison is made between analytical predictions and test results.

Sunshield Dynamics Modeling

Structural modeling techniques are being developed to predict sunshield dynamic behavior in the presence of membrane wrinkling. Thin-film membranes in a stress free state have negligible bending stiffness, but can be stress stiffened by applying in-plane tensile loads. The out-of-plane stiffness of the tensioned membrane is referred to as differential stiffness, and must be properly accounted for in structural models. In the case of the NGST sunshield design considered here, the out-of-plane structural stiffness is derived from the tensile loading applied at the membrane corners. An important characteristic of membrane behavior is wrinkling. Wrinkles are out-of-plane deformations that occur due to local buckling in regions of the membrane that develop compressive stresses. The geometry of structural wrinkles is dependent upon both the loading and the boundary conditions for the structure. Structural wrinkles must be adequately accounted for in sunshield models because their presence alters the stress distribution, and hence the differential stiffness of the structure.[4]

There are several approaches available for modeling wrinkled membrane structures, including: standard element formulations, the cable network method, and tension field theory methods. Modeling the thin-film membrane layers using standard membrane or plate elements in the presence of compressive stresses can lead to numerical problems during out-of-plane dynamics analyses and results may be inaccurate because the stress distribution in the membrane will not be represented properly. The cable

network method is a unique modeling technique that was developed specifically for modeling pretensioned, wrinkled membranes.[5] The approach is based on the established principle that load transfer in wrinkled regions takes place along wrinkle lines. Therefore, the membrane is meshed with a network of cables (preloaded bar elements) that is mapped to the wrinkle pattern of the structure. The mass of the membranes is distributed uniformly along connector cables that connect the load transfer cables in the network. Thus, the cable network model approximates both the load paths and mass distribution in the wrinkled structure. This approach is useful for determining the out-of-plane structural dynamic characteristics of pretensioned, wrinkled membrane structures. However, it is limited in that it requires prior knowledge of the wrinkle pattern to create the cable network and does not account for in-plane shear or thermal effects. The cable network method has been utilized to model the ISIS and one-tenth scale model NGST sunshields. A more accurate representation of membrane wrinkling can be obtained by using tension field theory in conjunction with standard finite elements to enforce 'no compression' membrane material behavior.[6,7] This approach can be used to accurately determine the state of stress in the membrane and the overall geometry of the wrinkled region; however, it does not provide results for the amplitude, wavelength, and number of the wrinkles. Advantages of this method include the prediction of wrinkle region geometry and a more accurate representation of in-plane membrane behavior (shear and thermal expansion effects). This approach is planned for use in future modeling and analysis efforts for studying the structural dynamic and thermal-structural behavior of the one-tenth scale model sunshield. In order to provide data for validating modeling techniques, a series of ground dynamic tests have been completed at NASA Goddard Space Flight Center using the one-tenth scale model NGST sunshield test article. The following section provides an overview of these tests.

Sunshield Dynamics Tests

The objectives of the one-tenth scale sunshield ground dynamic tests were: (1) to gather data for characterizing the dynamic behavior of a subscale model of the NGST sunshield for correlation with analytical models and (2) to validate instrumentation, excitation, and data processing routines for the ISIS flight experiment. A more comprehensive description of the test setup and results is provided in Refs. 8-9.

Overview of Dynamic Tests

The test article is a one-tenth scale model of the NGST sunshield yardstick design and was scaled down from the full-scale concept using constant thickness scaling laws.[10] The main components of the test article are a stiff aluminum central mounting block, four aluminum support tubes with their corresponding tip hardware, and four 13 micron thick Kapton® membranes. The test article is 3.4 m long by 1.52 m wide by 0.1 m thick, and has an overall weight of 4.1 kg. Figure 1 presents a schematic of the sunshield test article. At the tip of each tube is mounted a composite ladder structure that maintains a constant distance between the membrane layers. The membranes are attached at the corners to the constant force springs
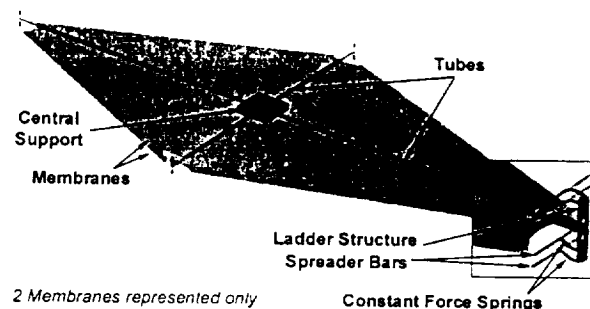
Figure 1: One-tenth scale model NGST sunshield test article.

using a composite spreader bar. At the root, the membranes are clamped to the central block between thin aluminum plates that maintain a constant spacing between the layers.

The test setup consists of the one-tenth scale model sunshield, a test stand to support the test article, an electrodynamic shaker, and the instrumentation suite. The sunshield is attached to the shaker armature at its central support and is excited by base driven
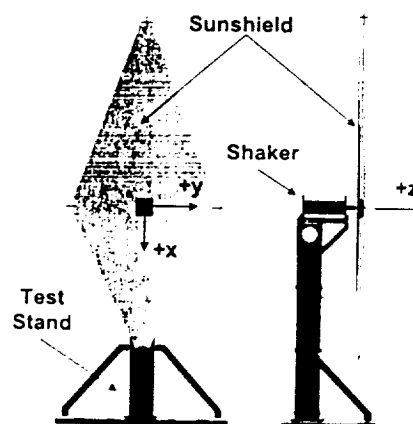
Figure 2: Schematic of test setup with sunshield in short side down orientation.

motions. Tests were completed with the sunshield in two orientations: short side down and long side down. The test setup for the short side down configuration is shown in Fig. 2.

Three types of tests were completed: (1) random excitation, (2) impulse excitation, and (3) sine dwell. The instrumentation suite for the tests consists of accelerometers, force gages, and a laser vibrometer. Tri-axial accelerometers are located at the tip of each tube, on the central block, and on the test stand. Force gages are located at the mounting points on the central block and at the test article/shaker interface point. The laser vibrometer is used to scan individual points on the outer membrane layer.

Summary of Test Results

The primary objective of the testing was to determine the dynamic characteristics (natural frequencies, damping, and mode shapes) of the sunshield. A detailed discussion of the test results is beyond the scope of this paper (see Refs. 8-9). Results obtained from tests with the sunshield in the short side down orientation will be briefly summarized here. Tables 2 and 3 present a summary of the natural frequencies and damping values for the short and long side down orientations of the sunshield. For both sunshield orientations, the dominant modes of the system are associated with the fundamental bending modes of the long and medium length support tubes.

Table 2: Summary of test-derived sunshield modes for short side down orientation.

Mode	Description	Frequency (Hz)	Damping (%)
1	Membranes	1.609	8.8
2	Membranes	1.841	5.6
3	Membranes	2.426	10.2
4	Long side of membranes/ Long tube	2.998	4.8
5	Long tube/ Long side of membranes	3.483	5.2
6	Long and medium tubes + Membranes	4.109	6.2
7	Medium tube / Short side of Membranes	5.074	6.4
8	Medium tube / Short side of membranes	5.962	3.2

For the short side down orientation, the long tube response is characterized by strong resonances at 3 and 3.5 Hz. The 3.0 Hz mode involves the center of the long side of the membranes moving in-phase with the tube, while the 3.5 Hz mode involves the membranes moving out-of-phase with the tube. The medium tube

response is dominated by modes at 5.1 and 6.0 Hz. The first of these modes involves the short side of the membranes moving in-phase with the medium tube, and the second mode has the membranes moving out-of-phase with the tube. Additionally, there are low frequency modes at 1.6 and 2.0 Hz associated with 'flapping' of the membrane edges. These modes do not couple strongly into the support structure response.

Table 3: Summary of test-derived sunshield modes for long side down orientation.

Mode	Description	Frequency (Hz)	Damping (%)
1	Long side of Membranes / Long tube	1.462	5.6
2	Membranes	2.319	6.9
3	Membranes	2.714	6.2
4	Long tube / Long side of membranes	3.395	2.9
5	Long and medium tubes + Membranes	4.093	5.1
6	Medium tube / Short side of membranes	4.501	3.1
7	Medium tube / Short side of membranes	5.477	2.5

For the long side down orientation, the long tube response is characterized by a single strong resonance at 3.4 Hz that involves the long side of the membranes moving out-of-phase with the tube. The medium tube response is dominated by modes at 4.5 and 5.5 Hz. The first of these modes involves the center of the short side of the membranes moving in-phase with the medium tube, and the second mode has the membranes moving out-of-phase with the tube. Additionally, there are low frequency modes at 1.2, 2.3, and 2.7 Hz associated with membrane response that does not couple strongly into the support structure response.
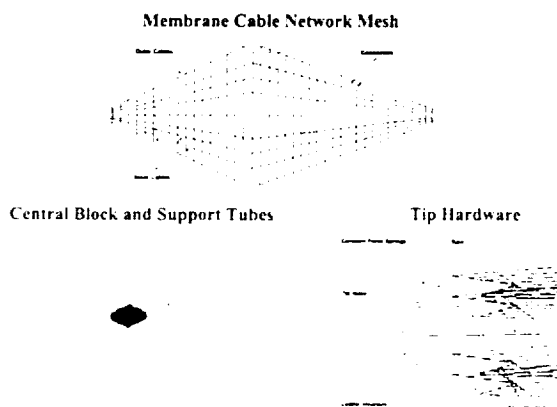
Analysis of Sunshield Dynamics

The following sections discuss an analysis of the one-tenth scale model NGST sunshield dynamics, including: the finite element model, analysis procedures, and results from modal, frequency response, and transient response analyses.

Finite Element Model

The finite element model for the one-tenth scale model NGST sunshield is presented in Fig. 3. The membrane layers are modeled with bar elements using the cable network method using the approach outlined in Ref. 5. The central block and shaker interface block are modeled using solid elements. The four support tubes are modeled using bar elements with

a nonstructural mass per unit length of 13.1 g/m included to represent the influence of the accelerometer cables. The support tubes are connected to central block via a common node and a rigid element that provides equivalent rotational stiffness at the interface. The ladder structure at the tips of the booms are modeled using massless bar elements, and the mass of the entire ladder structure and the attached instrumentation is represented using a concentrated mass of 34.1 g at the tip of each tube. The constant force springs (CFS) are modeled in two different ways with respect to the type of analysis: static or dynamic. In the static preloading analysis, the springs are modeled by applying forces that produce tension in the membranes and compression in the tubes. For a dynamic analysis, the CFS are modeled with rigid elements. In addition to the CFS loads, gravity loading was included since the ground tests showed that the dynamic response of the test article was different in the short and long side down orientations. Two support conditions were evaluated: fixed support and translating support. The fixed support model constrains the sunshield in all degrees of freedom (DOF 123456) at the attachment point of the test article to the shaker. The translating support case models the actual test setup by including the 0.4 Hz mode rigid body translational mode of the sunshield/shaker armature in the z-direction observed in the dynamic tests. For the translating support case, a simple two node shaker armature model consisting of a rigid element and a bar element is included. One node is at the attachment point of the sunshield to the shaker, while the other node is constrained in all degrees of freedom. The nodes are connected by a rigid element with dependent DOF 12456 and an element with stiffness in DOF 3 selected to reproduce the 0.4 Hz rigid body mode. It was necessary to model the support condition from the ground tests to provide representative analytical predictions for comparison with the test results.

Membrane Cable Network Mesh

Central Block and Support Tubes   Tip Hardware

Figure 3: One-tenth scale model NGST sunshield finite element model.

Analysis Procedure

Analyses performed to predict the dynamic behavior of pretensioned membrane structures involve two steps: (1) static analysis to calculate the differential stiffness resulting from preloading and (2) dynamic analysis of the preloaded structure. The preloading analysis of the structure was performed using a geometric nonlinear static solution with extraction of the final updated stiffness matrix representing the state of stress in the preloaded structure. The stiffness matrix extracted from the nonlinear static solution is then used to replace the standard stiffness matrix in all subsequent dynamic analyses. Alternately, the differential stiffness matrix could be recovered from the static analysis and added to the standard stiffness matrix in subsequent dynamic analyses. The finite element models are used to perform three types of dynamic analysis: modal, frequency response, and transient response. The modal analysis determines the natural frequencies and mode shapes for the structure. Additionally, mass participation factors are calculated to identify important modes (those having high mass participation). The frequency response analysis is used to predict the response of the test article to random excitation. The transient response analysis is a time domain calculation of the dynamic response of the structure and is used to predict the response of the test article to impulse excitation. Time-dependent acceleration profiles are applied to the structure and the response is recovered at points of interest. The following section presents results from a modal analysis of the sunshield.

Modal Analysis Results

A modal analysis was completed using the commercially available solver UAI/NASTRAN[11] to provide predictions for the natural frequencies and mode shapes of the sunshield. Four different cases were considered: (1) fixed support/short side down orientation, (2) fixed support/long side down orientation, (3) translating support/short side down orientation, and (4) translating support/long side down orientation. Comparison of results from the fixed and translating support cases shows that the sunshield frequencies differ by less than 5%; however, the mode shapes for the translating support case more closely resemble the measured mode shapes from the ground tests, thus the analytical predictions presented here will all be for the translating support case. Tables 3 and 4 summarize the results of the modal analyses for the short and long side down orientations of the sunshield. Significant modes were identified by considering the percentage of effective modal mass in the z and ry directions since these modes would contribute significantly to NGST observatory jitter.

Table 3: Summary of modal analysis results for short side down orientation.

Mode	Frequency (Hz)	% Z	% RY
1	0.395	100	9.67
2	2.1826	0.0022	9.67
14	3.3253	0.0001	11.05
18	3.5461	0.0007	41.32
30	4.7142	0.0000	3.64
43	5.5398	0.0000	14.54
59	6.4313	0.0000	9.49

Table 4: Summary of modal analysis results for long side down orientation.

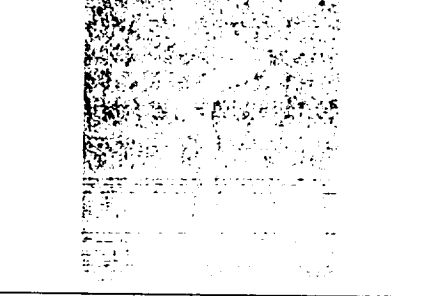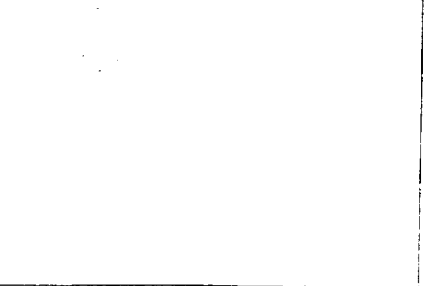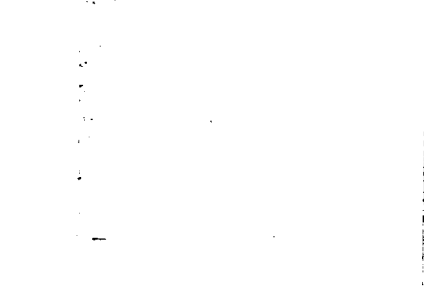| Mode	Frequency (Hz)	% Z	% RY
1	0.3951	100	0.66
6	2.6127	0.0009	17.73
10	2.8065	0.0005	0.39
18	3.6725	0.0004	48.05
34	4.7893	0.0000	4.31
47	5.5527	0.0000	13.27
55	6.3242	0.0000	8.91
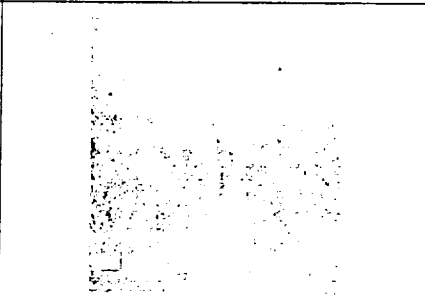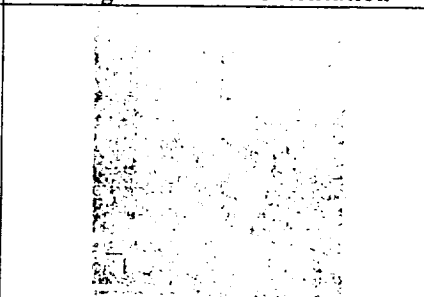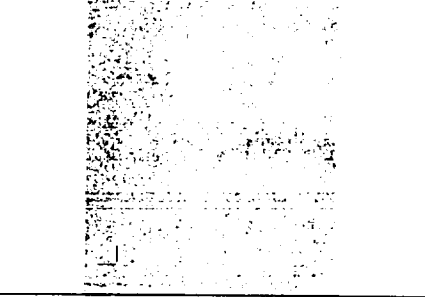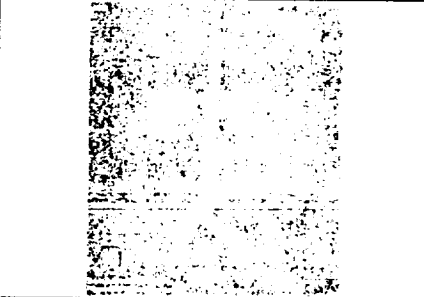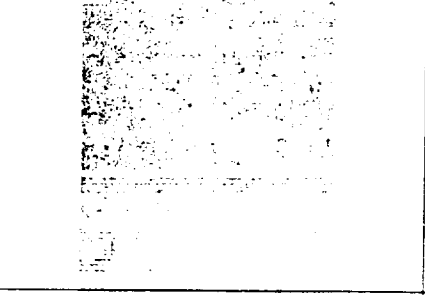
| Description	Short Side Down Orientation	Long Side Down Orientation
Long side of membranes with all four layers moving in-phase. Long tube moving out-of-phase with membranes. Frequency: Short side down: F = 2.18 Hz Long side down: F = 2.61 Hz		
First bending mode of long tube. Long side of membranes (central region moving out-of-phase with tube, tip region moving in-phase with tube). Frequency: Short side down: F = 3.54 Hz Long side down: F = 3.67 Hz		
First bending mode of medium tube. Short side of membranes: central region moving out-of-phase with tube / tip region moving in-phase with tube. Frequency: Short side down: F = 5.54 Hz Long side down: F = 5.55 Hz		
Bending mode of medium tube. Short side of membranes: central region moving in-phase with tube / tip region moving out-of -phase with tube. Frequency: Short side down: F = 6.43 Hz Long side down: F = 6.32 Hz		

Figure 4: Predicted mode shapes of significant sunshield modes.

Tables 3-4 summarize the frequencies and effective modal mass for each of the significant modes of the system. Note that mode 1 captures 100% of the modal effective mass in the z-direction. Recall that this 'shaker' mode involves the rigid body translation of the sunshield in the z-direction. The percentage of the effective modal mass inertia about the y-axis (I-YY) was used to select the significant 'flexible' modes of the system. For both the long and short side down orientations, the effective modal mass about the y-axis accounts for over 90% of the rigid body mass moment of inertia of the system. In both cases studies, there are seven significant modes. Mode 1 is the so-called shaker mode. The next two modes (between 2 and 3 Hz) are primarily associated with the membranes. The first mode involves all four layers on the long side of the membranes moving in-phase. This mode has predicted frequencies of 2.2 Hz in the short side down orientation and 2.6 Hz in the long side down orientation. The second mode involves all four layers on the short side of the membranes moving in-phase. This mode has predicted frequencies of 3.3 Hz in the short side down orientation and 2.8 Hz in the long side down orientation. Note that the frequency of these modes varies significantly depending on the orientation of the sunshield. The first bending mode of the long tube is at 3.55 Hz in the short side down orientation and 3.67 Hz in the long side down orientation. The first bending mode of the medium tube is at 5.54 Hz for the short side down orientation and 5.55 Hz for the long side down orientation. The remaining modes are associated with higher order membrane modes where all four membrane layers are moving in-phase and involve membrane-support tube interactions. Figure 4 presents plots of the mode shapes for the four flexible modes exhibiting the highest modal effective mass. Comparison between the predicted and measured frequencies and mode shapes is presented later in this paper. The following section discusses a transient dynamic analysis completed to simulate the results of the impulse excitation tests completed during ground testing of the sunshield.

Impulse Excitation Test Simulation

A transient response analysis was completed using the modal method in UAI NASTRAN (SOL 12) in order to simulate the impulse excitation tests performed on the sunshield. The translating support model was used in the analysis. Damping was included in the analysis using average values derived from the ground tests (see Tables 3-4). The loading was applied as a force at the shaker test article interface. The excitation profile utilized test results obtained from the force transducer at the test article shaker interface in order to closely simulate the tests. Results from the

analysis were recovered at nodes corresponding to measurement locations in the ground tests. Time histories were saved for the accelerometers, force gage, and laser measurement locations. These time history predictions were then post-processed using MATLAB to obtain frequency domain results that are comparable to those obtained in the ground tests. Figures 5-6 present the predicted transfer functions calculated using the force at the test article shaker force transducer location as the source and the tube acceleration or membrane velocity measurements as the response. Due to space considerations, predictions are presented here only for the short side down orientation of the sunshield. The predicted transfer functions for the long and medium tubes are presented in Fig. 5. The long tube response shows a large resonance at the frequency corresponding to its first bending mode. The medium tube response shows peaks at frequencies corresponding to the medium tube bending mode at 5.5 Hz and the short side of the membranes/medium tube mode at 6.5 Hz.
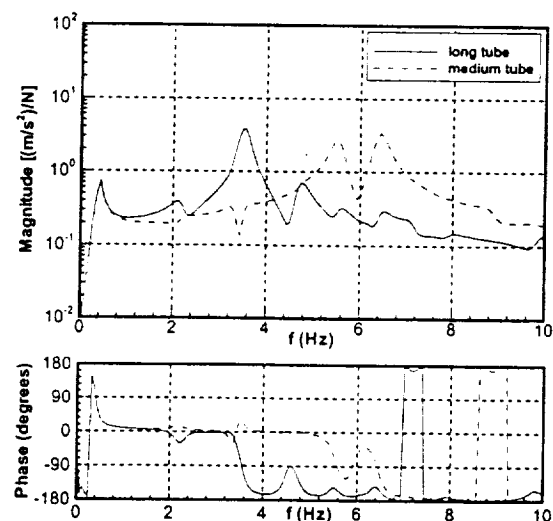
Figure 5: Predicted transfer functions for long and medium support tubes.

The predicted transfer functions for points on the long and short sides of the outer membrane layer are shown in Fig. 6. The point on the long side of the membrane has peaks at frequencies corresponding to 2.2, 3.5, and 4.7 Hz. The 2.2 Hz mode is associated with the first mode of the long side of the membranes with all four layers moving in-phase. The 3.5 Hz mode corresponds to the first bending mode of the long tube. The 4.7 Hz mode is a higher order mode of the long side of the membranes. Note that only the 2.2 Hz membrane mode does not couple significantly with the support structure as evidenced by the lack of corresponding peaks in Fig 4. The point on the short side of the membranes has major peaks at 3.3, 3.5, 5.5, and 6.4 Hz. The 3.3 Hz

mode is the first mode of the short side of the membranes with all four layers moving in-phase. The 3.5 Hz mode corresponds to the first bending mode of the long tube. Note that these peaks are nearly coincident and difficult to distinguish. The 5.5 Hz mode corresponds to the first bending mode of the medium tube. The 6.4 Hz mode corresponds to a higher order mode of the short side of the membranes. Note that while the first mode of the short side of the membranes does not couple significantly with the support tubes (as evidenced by the lack of a corresponding peak at 3.3 Hz in the tube FRF's), the higher order mode of the short side of the membranes couples significantly with the medium tube.
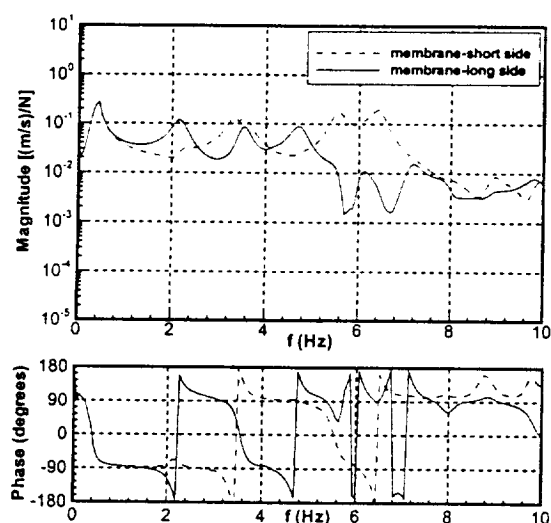
Figure 6: Predicted transfer functions for points on long and short sides of outer membrane layer.

In the next section comparisons are made between predictions from the finite element models and the results obtained from the ground tests.

Comparison of Analysis and Test

Predictions from the finite element analysis are now compared with results from the ground tests for the short side down orientation of the sunshield. Two types of comparisons will be made. First, the predicted frequencies and mode shapes from the modal analysis will be compared with the modal parameters determined from the random excitation tests and mode shapes captured during the sine dwell tests. Second, predictions from the transient response analysis will be compared with both time and frequency domain measurements from the impulse excitation tests.

Mode Shapes

The ground tests determined modal parameters (frequencies, damping values, and mode shapes) for the sunshield through two types of tests: random excitation and impulse excitation. The random and impulse excitation tests provided course mode shapes for the sunshield (only for the support structure for the impulse tests). Additionally, the sine dwell tests gave fine scale mode shapes but only for the outer membrane layer. First, comparison is made between the analytical predictions and results from the random excitation tests. A quantitative comparison between the predicted and measured mode shapes was obtained using the commercially available Dynaview software package[12] to perform orthogonality calculations. Finite element analysis predicts two low frequency membrane modes involving all four membrane layers moving in-phase. The ground tests identified four membrane modes between 1 and 3 Hz. Several of the measured modes appear to involve 'flapping' of the membranes, a phenomenon not predicted by the finite element model. Pairing of predicted and measured mode shapes was accomplished using the orthogonality calculations. A total of five pairs were obtained. Table 5 summarizes the results.

Table 5: Comparison of predicted and measured frequencies for mode shape pairs in short side down orientation.

Mode Pair	FEA (Hz)	Test (Hz)	% Difference
A	0.40	0.40	0.00
B	2.18	3.00	-27.33
C	3.55	3.48	+2.01
D	5.54	5.07	+9.27
E	6.43	5.96	+7.89

Mode pair A is the shaker mode and shows the highest degree of correlation of all the mode pairs (orthogonality = 1.0). The next mode pair involves the first mode of the long side of the membranes with the long tube moving in-phase with the membranes. The predicted and measured frequencies differ significantly, however the orthogonality calculation is 0.79. Both the analysis and the tests show the presence of a mode involving membrane-tube interaction between the long and medium tube modes, however the modes correlated poorly and are not included as a pair. Mode pair C is the first bending mode of the medium tube with the central region of the long side of the membranes moving out-of-phase with the tube. For this pair, the predicted and measured frequencies differ by only 2% and the orthogonality calculation gives a result of 0.75. Mode pairs D and E are both dominated by interactions

between the medium tube and the short side of the membranes. Mode pair D involves the first bending mode of the medium tube with the short side of the membranes (tip region) moving in-phase with the tube. Additionally, the analytical model predicts twin lobes in the central region of the short side of the membranes moving out-of-phase with the tube that are not evident in the measured results. The predicted and measured frequencies differ by 9% and the orthogonality calculation gives a result of 0.74. Mode pair E again involves a bending mode of the medium tube, however in this mode the short side of the membranes (tip region) are moving out-of-phase with the tube. The analytical model additionally predicts the presence of twin lobes in the central region of the short side of the membranes moving in-phase with the tube that are not seen in the measured results. The difference is frequencies is 8% and the orthogonality calculation gives a result of 0.56. In general, the orthogonality calculations showed only fair correlation between the predicted and measured mode shapes. The support tube dominated modes show good correlation, while the membrane dominated modes show poor correlation. One difficulty is the limited number of membrane measurement points available for comparison with the finite element model predictions.

Figure 7 presents a comparison between the predicted mode shapes and the velocity contours obtained from the sine dwell tests for the outer membrane layer. The sine dwell tests were completed at slightly different frequencies than those obtained from analysis of the results from the random excitation tests. Qualitative comparison is made here between the predicted mode shapes and the measured velocity contours. The first comparison is for the first mode of the long side of the membranes. Recall that the analytical model predicts a frequency of 2.2 Hz for this mode, while the random excitation tests showed a frequency of 3.0 Hz. Sine dwell tests were completed at 2.3 and 3.0 Hz. The velocity contour from the sine dwell test completed at 2.3 Hz compares more favorably with the predicted mode shape at 2.2 Hz than the 3.0 Hz test results. The next comparison is for the first bending mode of the long tube. The results show good agreement with both predicting a central region out-of-phase with the outside edges. The next two comparisons are for the modes involving interactions between the medium tube and the short side of the membranes. There are only small differences between the outer membrane layer mode shapes for these modes. The predicted and measured shapes both show that the response is greatest on the short side of the membranes. The predicted mode shapes include a pair of lobes in the central region of the membrane that are out-of-phase with the tip region, however the test results do

not include this feature. The velocity contours obtained from the sine dwell tests compare favorably with the mode shapes predicted by the finite element model on a qualitative level. Future work will involve performing a quantitative comparison between the predicted mode shapes and the results obtained from the sine dwell tests.

Impulse Test Simulation

Figures 8 – 9 present a comparison of the predicted and measured response of the sunshield in both the time and frequency domains. Figure 8 provides results for the response at the tip of the long support tube. The predicted and measured acceleration in the out-of-plane (z) direction at the tip of the tube as a function of time is presented in Fig. 8(a). The predicted response shows similar peak acceleration levels and decay time to the measured response. Figure 8(b) provides a comparison of the predicted and measured frequency response functions (FRF's) for the long and medium support tubes. The FRF's were calculated using the drive point force as the input and the acceleration at the tip of the long tube as the output. The FRF's show similar results in terms of the magnitude and frequency of the peaks. The major difference is for the medium tube/short side of the membranes modes where the analysis predicts two strong peaks at 5.5 and 6.5 Hz, while the measured FRF shows a strong peak at 6.0 Hz and a smaller peak at 4.8 Hz. Figure 9 provides results for the response at points on the long and short sides of the outer membrane layer. The predicted and measured out-of-plane velocity for a point on the long side of the membrane as a function of time is shown in Fig. 9(a). The analytical predictions show similar peak velocity values and decay time to the measured results. Figure 9(b) compares the predicted and measured frequency response functions (FRF's) for the points on the long and short sides of the outer membrane. The FRF's were calculated using the drive point force as the input and the membrane velocity as the output. The results are less consistent than for the support tubes. The measured FRF's show more peaks than the analytical model predicts. Both the measured and predicted FRF's for the long side of the membrane show peaks at 2.2, 3.5, and 4.5 Hz. The measured FRF shows additional peaks at 1.7, 2.5, and 6.5 Hz. The predicted FRF for the short side of the membrane shows peaks at approximately 3.4, 5.5, and 6.5 Hz, while the measured FRF has peaks at 1.9, 3.3, 3.9, 5.0, and 6.0 Hz. In general, the analytical model performed well in simulating the response of the test article to impulse excitation.
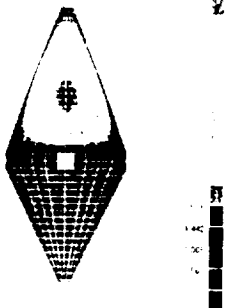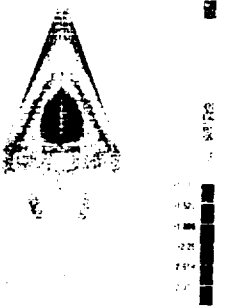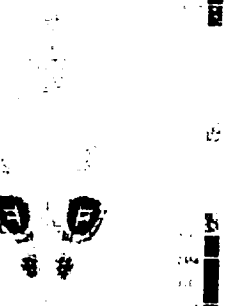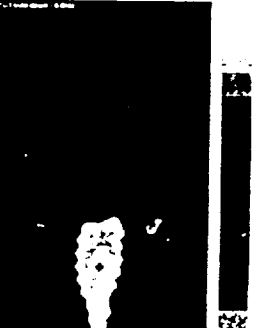
8
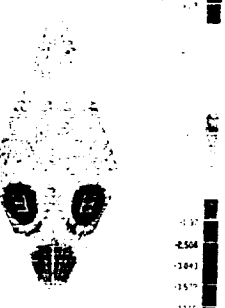
Description	Predicted	
Long tube/Long side of membranes Frequency: Predicted: F = 2.2 Hz Measured: F = 2.3 Hz		
Long tube/Long side of membranes Frequency: Predicted: F = 3.5 Hz Measured: F = 3.5 Hz		
Medium tube/Short side of membranes Frequency: Predicted: F = 5.5 Hz Measured: F = 5.1 Hz		
Medium tube/Short side of membranes Frequency: Predicted: F = 6.4 Hz Measured: F = 6.0 Hz		

Figure 7: Comparison of predicted mode shapes and measured velocity cont   side down orientation of sunshield.

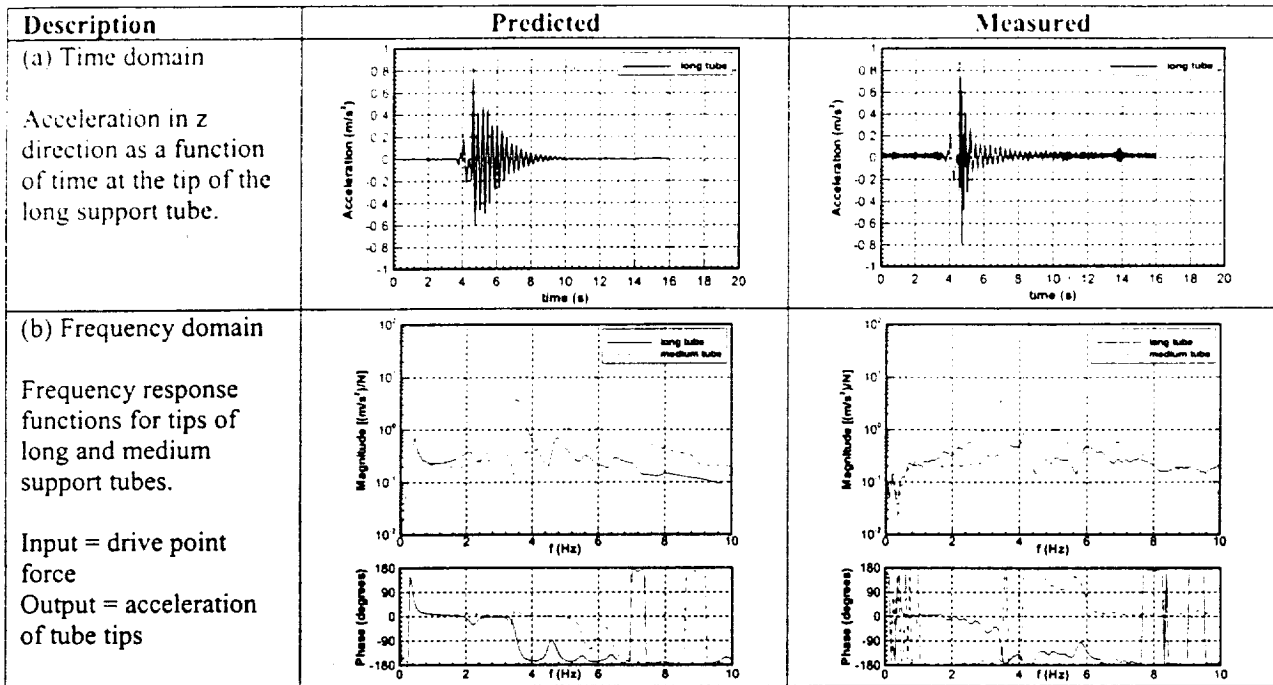| Description	Predicted	Measured
(a) Time domain Acceleration in z direction as a function of time at the tip of the long support tube.		
(b) Frequency domain Frequency response functions for tips of long and medium support tubes. Input = drive point force Output = acceleration of tube tips		

Figure 8: Comparison of predicted and measured response of sunshield support tubes to impulse excitation: (a) time domain response and (b) frequency domain response.

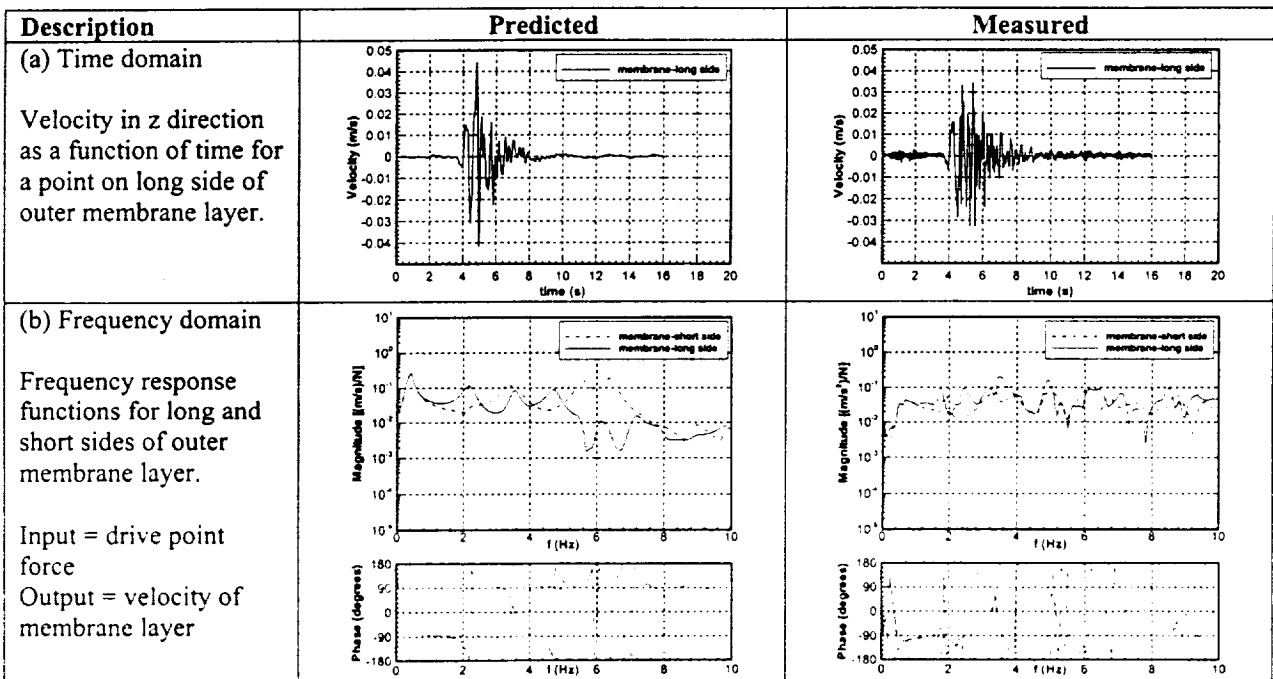| Description	Predicted	Measured
(a) Time domain Velocity in z direction as a function of time for a point on long side of outer membrane layer.		
(b) Frequency domain Frequency response functions for long and short sides of outer membrane layer. Input = drive point force Output = velocity of membrane layer		

Figure 9: Comparison of predicted and measured response of points on outer membrane layer of sunshield to impulse excitation: (a) time domain response and (b) frequency domain response.

Conclusions

The structural dynamic behavior of a subscale model of the NGST sunshield was investigated through analytical and experimental studies. A finite element model of the sunshield was developed using the cable network method to represent wrinkled membrane behavior. Dynamic analyses were performed using the UAI NASTRAN finite element solver to simulate the behavior of a one-tenth scale model sunshield during ground testing. An overview of the test setup and representative results from ground testing was presented, and results from the ground tests were then compared with analytical predictions from the finite element model. Natural frequencies and mode shapes obtained from the random excitation and sine dwell tests were correlated with analytical predictions from the modal analysis. In general, the analytical predictions compared favorably with the test results. The difference between the predicted and measured natural frequencies ranged from 2 to 27%. The predicted mode shapes correlated well for the modes dominated by the support tubes, while the membrane dominated modes showed less satisfactory agreement. The impulse excitation tests were simulated using a transient response analysis. Analytical predictions were compared with test results in both the time and frequency domains. The time domain predictions compared well with the measured results showing similar peak levels and decay times. Frequency response functions calculated from the predicted and measured time domain results using identical processing techniques also demonstrated good agreement. In conclusion, a test validated approach for modeling and analyzing the structural dynamics of the NGST sunshield has been successfully demonstrated. This approach is applicable to a broad range of tensioned membrane structures representative of those planned for future gossamer spacecraft.

References

1. L. Pacini and M. C. Lou, "Next Generation Space Telescope (NGST) Pathfinder Experiment: Inflatable Sunshield In Space (ISIS)," October 1999, SAE 1999-01-5517.

2. J. Carey, and D. Cadogan, et. al, "Inflatable Sunshield In Space (ISIS) Versus Next Generation Space Telescope (NGST) Sunshield – A Mass Properties Comparison," April 3-6, 2000, AIAA-2000-1569.

3. Lienard, S., Johnston, J.D., Adams, M.L., Stanley, D., Alfano, J.P., Romanacci, P., "Analysis and Ground Testing for Validation of the Inflatable Sunshield in Space (ISIS) Experiment", *Proceedings of the 41st AIAA ASME ASCE AHS ASC Structures, Structural Dynamics, and Materials Conference,* Atlanta, GA, 3-6 April, 2000, AIAA Paper AIAA-2000-1638.

4. Fang, H.F and Lou, M.C., "Analytical Characterization of Space Inflatable Structures – An Overview," 40th AIAA Structures, Structural Dynamics, and Materials Conference, St. Louis, MO, Paper No. AIAA-99-1272, April 1999.

5. Lienard, S.L., "Characterization of Large Thin Film Membrane Dynamic Behavior with UAI-NASTRAN Finite Element Solver," SAE Paper 199-01-5518, October 1999.

6. Adler, A.L., Mikulas, M.M., and Hedgepeth, J.M., "Static and Dynamic Analysis of Partially Wrinkled Membrane Structures," 41st AIAA Structures, Structural Dynamics, and Materials Conference, Atlanta, GA, Paper No. AIAA-2000-1810, April 2000.

7. L., Xinxiang, Jenkins, C., and Schur, W., "Fine Scale Analysis of Wrinkled Membranes," to appear in International Journal of Computational Engineering and Science, 2000.

8. Lienard, S., Johnston, J., Ross, B., and Smith, J., "Dynamic Testing of a One-Tenth Scale NGST Sunshield in a Vacuum Environment – Test Report," NASA Goddard Space Flight Center, February 2001.

9. Lienard, S., Johnston, J., Ross, B., and Smith, J., "Dynamic Testing of a Subscale Sunshield for the Next Generation Space Telescope (NGST)," Submitted to: AIAA Gossamer Spacecraft Forum, Seattle, WA, April 16-19, 2001.

10. Greschik, G. and Mikulas, M.M., "Scale Model Testing of Nonlinear Phenomena With Emphasis on Thin Film Deployable Structures," IUTAM-IASS Symposium on Deployable Structures: Theory and Applications, Cambridge, UK, September 1998.

11. UAI NASTRAN User's Guide for Version 20.0, Universal Analytics, Inc., Torrance, CA, 1997.

12. Dynaview for Windows User's Manual for Version 2.2, Practical Systems and Technology.